Effect of interference between two colored noises on the stationary states of a Brownian particle

Shrabani Mondal and Bidhan Chandra Bag*
Department of Chemistry, Visva-Bharati, Santiniketan 731 235, India
(Received 24 November 2014; published 30 April 2015)

In this paper we present properties of an external colored cross-correlated noise-driven Brownian system which is coupled to a thermal bath. Multiplicative cross-correlated noises can stabilize the transition state. Thus by monitoring the interference between the noises one can understand the mechanism of a chemical reaction. At the same time, we have investigated how the interference affects the barrier-crossing dynamics. In its presence breakdown of the Arrhenius result occurs. The breakdown becomes prominent if the multiplicative noises become additive in nature. We have also investigated how the power law behavior of the rate constant as a function of damping strength is affected by the properties of external colored noises. Furthermore, we have observed that multiplicative colored cross-correlated noises can induce the resonant activation phenomenon.

DOI: 10.1103/PhysRevE.91.042145 PACS number(s): 02.50.Ey, 05.40.−a

I. INTRODUCTION

Study of noise-driven dynamical systems has long been the focal theme in the field of statistical mechanics, simply because of its potential applications in physics, chemistry [1–6], biology [7–9], economics [10], social sciences [11–13], etc. One of the key areas of the stochastic processes is the activated barrier-crossing dynamics which is an important issue in chemistry and condensed matter physics. In this context the system may be thermodynamically closed [14,15] or open [16,17,18–22]. When a stochastic system is thermodynamically made open by the action of external periodic or random forces, significant changes in the dynamics take place which reflect the constructive role of noise in dynamical systems. The well-known examples include stochastic resonance [16,23,24], resonant activation [15,17,18,19,22,25], noise-induced transition [26], ratchet and rectification of noise [27], etc., to mention a few. In these issues more than one noise may be relevant. If the noises are from the same origin, then they may be cross-correlated [28,29]. Noises of this kind have attracted strong interest in the recent past in different contexts. The effect of cross-correlation has been considered in different contexts such as relaxation time in a bistable system [30,31], a single-mode laser dynamics [32], bistable kinetics [33], transport of particles [34], stochastic resonance [23,35], effect of environment on the growth of cancer cells [36], entropy production [37], splitting of the Kramers rate in a symmetric triple well potential [20], and others [31,38]. In Ref. [31], the authors have pointed out that the cross-correlated noises may appear in the system in different ways. Keeping this in mind, in the present paper we have considered a colored cross-correlated noise-driven nonlinear dynamical system. To make the present study general we have also considered the that noises may be either additive or multiplicative in nature. The specific aim is to investigate the role of interference of colored multiplicative noises on the stationary states of the Brownian system. We have shown that multiplicative cross-correlated noise can stabilize the transition state. In other words, the transition state becomes intermediate like in the presence of cross-correlated multiplicative noises. Thus it is possible to understand the mechanism of a chemical reaction by controlling the cross-correlation behavior between the multiplicative noises. In Ref. [39] the authors have shown that study of intermediate is important to understand protein folding kinetics. We have also addressed another issue. How do the properties of the Brownian particle change if the multiplicative noises become additive in their characteristics? We have explored these issues based on the Fokker-Planck description of the stochastic process. Our investigation shows that colored cross-correlation between the multiplicative noises can induce resonant activation. Another point to be mentioned here is that comparing the present calculation with the earlier studies in Refs. [40,41] one may conclude that the present method is a unified approach.

Before leaving this section we would like to mention the relevance of the present study. A photosensitive thermal reaction of a carbonyl compound ($R_2C=O$, R may be an alkyl or aryl group, and it may also be hydrogen) with an acid, HX (X refers to halogens), in the presence of a fluctuating electric field may mimic the present model study. For the chemical reaction with lowest potential energy path, it is necessary to break π bond in $R_2C=O$ and dissociation of the HX bond. In the next step, atoms are recombined to from a stable compound, $R_2C(OH)X$. The reaction coordinate comprises both bond-breaking and -making processes. The reaction path with minimum potential energy suggests a double-well potential in terms of the reaction coordinate. One of the wells is for the reactant side, and the another well corresponds to the product side. However, one may carry out the present chemical reaction in the presence of electric fields. One of the fields will break the π bond in $R_2C=O$, and another will break the σ bond in HX molecules. In an experimental situation one may introduce a light field of fluctuating intensity which polarizes the photosensitive carbonyl group to speed up a chemical reaction. If an electric field of fluctuating intensity of common origin is now imposed, in addition, on the polarized system, then the rate of nucleophilic attack of X^- will depend on the cross-correlation between the fluctuating light and electric fields. Thus the chemical reaction may take place in the presence of two cross-correlated noises. Now, we would like to mention how one can generate the cross-correlated electric fields experimentally. It is well known that one can generate fluctuating voltage from ambient energy through piezoelectric materials [22]. If a coil is coupled to

*bidhanchandra.bag@visva-bharati.ac.in

this device, then fluctuating magnetic as well as electric fields will be generated. Electric fields having a wide spectrum may be created here. Because of the common origin, any two fluctuating fields may be cross-correlated. Thus the proposed chemical reaction may be carried out experimentally.

The present model study may also be important in the context of barrier-crossing dynamics in biology such as chemical reactions in cell and protein-folding dynamics. A barrier-crossing system experiences a fluctuating force due to direct coupling with its immediate surroundings via a strong chemical bond. At the same time, the system also experiences a random force from the thermal bath of biological fluids. The fluctuating force from the direct coupling may be influenced by the thermal bath. Thus the fluctuating forces acting on the barrier-crossing system may be cross-correlated.

The outline of the paper is as follows: In Sec. II we present the model and general aspects. The barrier-crossing rate has been calculated in Sec. III. The paper is concluded in Sec. IV.

II. THE MODEL AND GENERAL ASPECTS

To begin, we consider a noise-driven dynamical system at an overdamped limit. The corresponding Langevin equation of motion for a Brownian particle with mass, $m = 1$, can be written as

$$\frac{dq}{dt} = -V'(q)/\gamma + q\eta_1(t)/\gamma + q\eta_2(t)/\gamma + \zeta(t)/\gamma. \quad (1)$$

Here the prime denotes the derivative with respect to position (q). For the present problem we have chosen the potential energy function, $V(q) = aq^4 - bq^2$. We now define all the noises in Eq. (1). η_1 and η_2 are Gaussian colored noises, and their two time correlation functions are $\langle \eta_1(t)\eta_1(t')\rangle = \frac{D_1'}{\tau_1} e^{\frac{-|t-t'|}{\tau_1}}$, $\langle \eta_2(t)\eta_2(t')\rangle = \frac{D_2'}{\tau_2} e^{\frac{-|t-t'|}{\tau_2}}$, and $\langle \eta_1(t)\eta_2(t')\rangle = \langle \eta_2(t)\eta_1(t')\rangle = \frac{\lambda\sqrt{D_1'D_2'}}{\tau} e^{\frac{-|t-t'|}{\tau}}$, respectively.

Here λ measures the strength of interference between the colored noises and τ is the correlation time for the cross-correlation. The remaining noise in Eq. (1) is a white Gaussian thermal noise, and it is related to the damping strength of the thermal bath through the standard fluctuation-dissipation relation, $\langle \zeta(t)\zeta(t')\rangle = 2\gamma k_B T\delta(t-t')$. T is the temperature of the thermal bath. We now replace two multiplicative noises by an effective noise [31], η,

$$\eta(t) = \eta_1(t) + \eta_2(t). \quad (2)$$

Then one can write the two time correlation function for η as

$$\langle \eta(t)\eta(t')\rangle = \frac{D_e}{\tau_e} e^{\frac{-|t-t'|}{\tau_e}}, \quad (3)$$

where

$$D_e = \int_0^\infty \langle \eta(t)\eta(0)\rangle\, dt = D_1 + 2\lambda\sqrt{D_1 D_2} + D_2 \quad (4)$$

and

$$\tau_e = \int_0^\infty t\,\langle \eta(t)\eta(0)\rangle\, dt = \frac{D_1\tau_1 + 2\lambda\sqrt{D_1 D_2}\tau + D_2\tau_2}{D_e}. \quad (5)$$

In the above two equations we have used $D_1 = D_1'/\gamma^2$ and $D_2 = D_2'/\gamma^2$.

Based on Eqs. (2)–(5), it seems that use of two noise terms in Eq. (1) may create confusion. Here we should mentione that if each noise renders an independent parameter like D_1 to the effective description of the system, then we cannot avoid the existence of the individual parameters. For example, in the proposed chemical reaction, η_1 may be used to break the π bond in $R_2C = O$. The related parameters for this process are D_1 and τ_1. They have a specific role to control the chemical reaction. Another noise, η_2, may be used to dissociate the HX molecule. For this part the related parameters are D_2 and τ_2. These parameters also posses a specific role. If the two noises are correlated (depending upon the nature of the source of the fluctuating electric fields), then there may be parameters like λ and τ. They have a role to control both processes. Thus Eq. (1) takes care of the importance of all the individuals. For a mathematically convenient description we have replaced the two noises by an effective noise, η. Any property of η should be a function of all the above mentioned parameters. By virtue of this one may identify the role of the properties of the individual noise to control the chemical reaction in the effective single noise description. To be mentioned here is that the replacement of two noises by an effective single noise has been adopted earlier in different contexts [31]. Another point to be mentioned is that in the cross-correlated noise-driven model system it has been assumed that one of the noises is multiplicative in nature [35–37]. But in reality both noises may be either additive or multiplicative in their characteristics. Then one may apply the present method to study these kinds of systems. Finally, even if a system is driven by a multiplicative colored noise and an additive thermal noise, then the present study is also applicable to this system according the effective single noise description. Then D_e and τ_e would be the characteristic parameters of the single noise. The multiplicative colored noise may correspond to the fluctuating light field which may induce the photochemical reaction. Organic photochemistry in the presence of a single electric field is well known. Thus the present model study is a general one.

To describe the colored noise-driven dynamical system different approximate methods have been developed such as the unified colored noise approximation (UCNA) scheme [4,42–44]. This scheme has been justified as a reliable Markovian approximation by means of a path integral technique [45]. Based on the interpolation procedure an extension of the unified colored noise description has been done for an additive colored noise-driven system in Ref. [46]. Shortly we will use the result of this approach. To study the present problem based on the effective Fokker-Plank description of the colored multiplicative noise-driven system, we have used the UCNA into Eq. (1). Then it becomes

$$\frac{dq}{dt} = \frac{[-V'(q)/\gamma + q\eta_0(t) + \zeta(t)/\gamma]}{A}, \quad (6)$$

where

$$A = 1 - \tau_e[h'(q) - h(q)/q]. \quad (7)$$

In the above equation we have used $h(q) = -\frac{1}{\gamma}\frac{d}{dq}V(q)$. The multiplicative noise, η_0, in Eq. (6) is a Gaussian white noise.

Then the two time correlation function for it is given by $\langle \eta_0(t)\eta_0(t')\rangle = 2D_e\delta(t-t')$.

Now the equivalent description corresponding to the Langevin equation (6) can be written as [23]

$$\frac{\partial\rho(q,t)}{\partial t} = -\frac{\partial}{\partial q}\frac{h(q)\rho(q,t)}{A} + D_e\frac{\partial}{\partial q}\frac{q}{A}\frac{\partial}{\partial q}\frac{q\rho(q,t)}{A} + D_T\frac{\partial}{\partial q}\frac{1}{A}\frac{\partial}{\partial q}\frac{\rho(q,t)}{A}, \tag{8}$$

where $D_T = \frac{k_BT}{\gamma}$. If the correlated noises are additive in nature, then the above equation becomes

$$\frac{\partial\rho(q,t)}{\partial t} = -\frac{\partial}{\partial q}\frac{h(q)\rho(q,t)}{A} + (D_e+D_T)\frac{\partial}{\partial q}\frac{1}{A}\frac{\partial}{\partial q}\frac{\rho(q,t)}{A}. \tag{9}$$

A in the above equation can be read as

$$A = 1-\tau_e h'(q). \tag{10}$$

From Eq. (6), it seems that we have deviated from the original problem, which is the colored noise-driven dynamical system. Here we should give probable justification for the acceptance of the Markovian description (6). For this we consider a simple case, the additive Ornstein-Uhlenbeck noise-driven harmonic oscillator. Based on the exact calculation the variance (σ_{q^2}) of the position variable is given by

$$\sigma_{q^2} = \frac{D_e\gamma^2}{(\gamma+\tau_e\omega_0^2)\omega_0^2}, \tag{11}$$

where ω_0 is the frequency of the harmonic oscillator. At the limiting condition where $\tau_e \to 0, \lambda = 0, D_2' = 0$, and $D_1' = \gamma k_BT$, the above equation becomes

$$\sigma_{q^2} = \frac{k_BT}{\omega_0^2}. \tag{12}$$

This is the well-known standard result. We would like to note that the unified colored noise approximation also gives the same result as given by Eq. (11). Thus the effective Markovian description is an exact one for the additive Ornstein-Uhlenbeck noise-driven harmonic oscillator. Shortly we will present further verification of the approximation scheme through the calculation of a probability distribution function for a nonlinear system which is driven by multiplicative noises.

We now mention some of the signatures of the colored noise-driven Brownian motion. Equation (6) suggests that the potential energy function is modified by $A(q)$, which is a function of the noise correlation time. The effective potential energy function [$V_{\rm eff}(q)$] is given by

$$V_{\rm eff}(q) = \int_0^q \frac{4aq'^3 - 2bq'}{A(q')}\,dq'. \tag{13}$$

The colored noise-driven motion is more correlated compared to the white noise-driven case. This implies that the colored noise itself can introduce a sense of additional quasideterministic force compared to its counterpart. Therefore it is apparent in the above equation that the deterministic force derived from the potential energy function may be affected by the noise memory-induced quasideterministic correlated motion. For a colored thermal noise-driven system, an effective potential energy function exists in the effective Markovian description in terms of the system coordinate and an auxiliary variable corresponding to the thermal noise [47]. However, the effective potential energy function for an additive colored noise-driven harmonic oscillator system is given by

$$V_{\rm eff}(q) = \frac{\omega_0^2q^2}{2A}, \tag{14}$$

where $A = 1+\tau_e\frac{\omega_0^2}{\gamma} > 1$. The above relation implies that the frequency of the harmonic motion is suppressed more as the noise correlation time grows. This suggests that the noise memory-induced quasideterministic force opposes the deterministic force derived from the potential energy function. According to the suppression of frequency of the harmonic potential, one may expect that the variance of the position variable would increase as the correlation time of the noise grows. But Eq. (12) suggests that σ_{q^2} decreases with an increase in τ_e. This anomaly can be resolved considering the effect of the noise correlation time on the diffusion constant. It decreases [as explicitly indicated in Eq. (9)] due to the noise memory-induced correlated motion. The role of this decrease on the change of the variance as a function of the noise correlation time may dominate over the other effect. It is the reason for the decrease of σ_{q^2} with increase in τ_e in spite of the suppression of the frequency of the harmonic potential.

To have further insight one may rearrange the Fokker-Planck equations (8) and (9) into the following forms:

$$\frac{\partial\rho(q,t)}{\partial t} = -\frac{\partial}{\partial q}\left\{\left[\frac{h(q)}{A}+\frac{D_eq}{A^2}\right] - \frac{A'}{A}\left(\frac{D_eq^2}{A^2}+\frac{D_T}{A^2}\right) - \frac{\partial}{\partial q}\left(\frac{D_eq^2}{A^2}+\frac{D_T}{A^2}\right)\right\}\rho(q,t) \tag{15}$$

and

$$\frac{\partial\rho(q,t)}{\partial t} = -\frac{\partial}{\partial q}\left[\frac{h(q)}{A} - A'\frac{(D_e+D_T)}{A^3} - (D_e+D_T)\frac{\partial}{\partial q}\frac{1}{A^2}\right]\rho(q,t). \tag{16}$$

The above equations are explicit description of the effect of noise properties on the drift and diffusion terms. If the noises are additive and white, then they have no contribution to the drift term. However, one may realize the signature of the noise properties through the following stationary solutions (ρ_{eqm} and ρ_{eqa}) of the above Fokker-Planck equations for additive and multiplicative noises,

$$\rho_{eqm}(q) = \frac{NA(q)^2}{(D_eq^2+D_T)} \times \exp\left(\int_0^q\left\{\frac{[h(q')A(q')+D_eq']}{(D_e'q^2+D_T)} - \frac{A'}{A}\right\}dq'\right) \tag{17}$$

and

$$\rho_{eqa}(q) = \frac{NA(q)^2}{(D_e+D_T)}\exp\left\{\int_0^q\left[\frac{h(q')A(q')}{(D_e+D_T)} - \frac{A'}{A}\right]dq'\right\}, \tag{18}$$

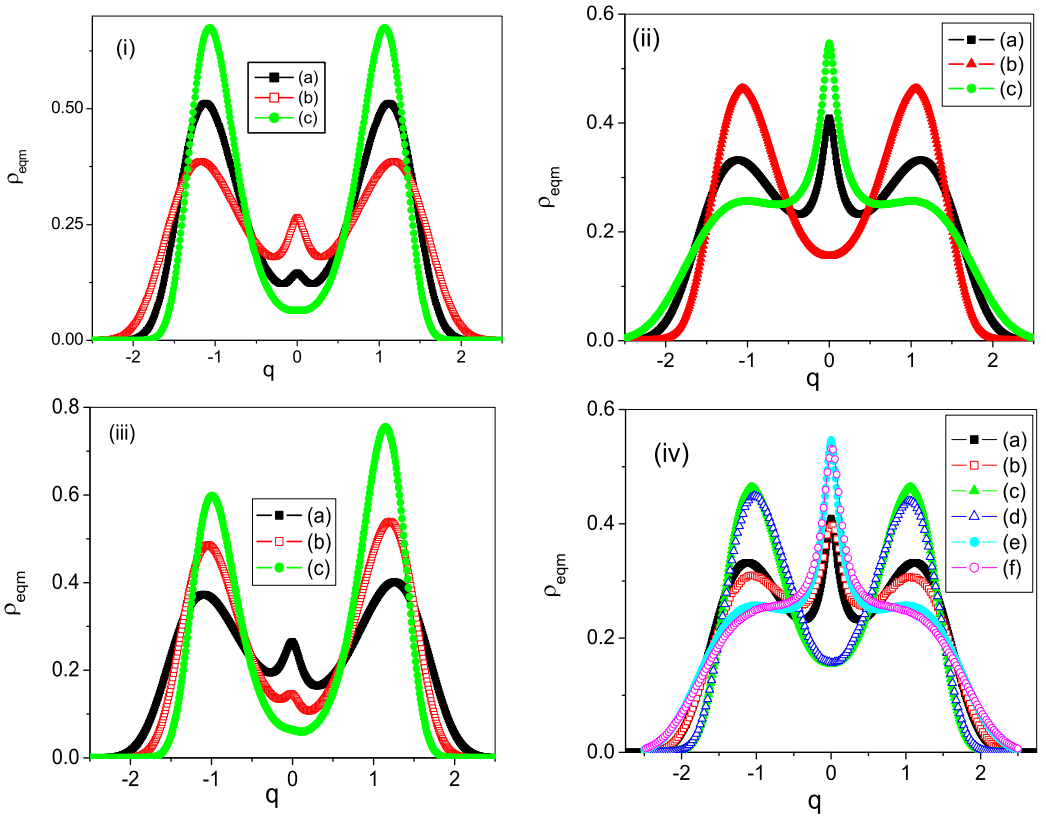

FIG. 1. (Color online) Plot of distribution function vs coordinate for common parameter set $a = 0.25, b = 0.5, \gamma = 1.0$ and the following cases: (i) $k_BT = 0.05, d_1 = d_2 = 1.0, \tau_1 = \tau_2 = 5.0$ (a) $\tau = 5.0, \lambda = 1.0$; (b) $\tau = 0, \lambda = 1.0$; (c) $\tau = 0, \lambda = 0.0$. (ii) $k_BT = 0.01, d_1 = d_2 = 0.5, \tau_1 = \tau_2 = 1.0$ (a) $\tau = 1.0 = \lambda$; (b) $\lambda = \tau = 0.0$; (c) $\lambda = 1.0, \tau = 0.0$. (iii) $c = 0.05, k_BT = 0.05, d_1 = d_2 = 1.0, \tau_1 = \tau_2 = 5.0$, (a) $\tau = 5, \lambda = 1.0$; (b) $\tau = 0, \lambda = 1.0$; (c) $\tau = 0, \lambda = 0.0$. (iv) (a) Theoretical, same set of parameters as in (ii) (a); (b) simulation, same set of parameters as in (ii) (a); (c) theoretical, same set of parameters as in (ii) (b); (d) simulation, same as in (ii) (b); (e) theoretical, same set of parameters as in (ii) (c); (f) simulation, same set of parameters as in (ii) (c) (units are arbitrary).

respectively. N in the above equations corresponds to the normalization constant for the respective cases. To check the validity of the present calculation we consider the limiting situation, $D_e = 0$ and $\tau_e = 0$. Then both probability distribution functions reduce to the following form:

$$\rho_{eq}(q) = N \exp\left[-\frac{V(q)}{k_BT}\right]. \tag{19}$$

Thus our calculation reproduces the standard result. We now explore how the distribution function depends on characteristics of the noises.

A. Cross-correlated colored noise-induced stabilization of transition state

We have calculated the probability distribution function using Eq. (17). The trapezoid rule with the integration step length, 0.01, has been used to find the distribution function as a function of the coordinate. We have checked that the numerical results are superposed for both step lengths, 0.01 and 0.005, respectively. With this check we have plotted the numerical results in Fig. 1 for several sets of parameters for the multiplicative noise (MN)-driven case. For this figure we have used $a = 0.25, b = 0.5, \gamma = 1.0$. Figure 1 suggests that by controlling the strength of cross-correlation among the multiplicative colored noise, the particle can be localized at the transition state corresponding to the double-well potential energy function. Even the probability of finding the particle may be maximum at the barrier top as implied in Fig. 1(ii). At the same time, we have demonstrated in Fig. 1(iii) that how the distribution function for the following asymmetric potential energy function depends on the characteristics of the multiplicative colored noises:

$$V(q) = aq^4 - bq^2 - cq^3. \tag{20}$$

The particle also can be localized at the transition state corresponding to the asymmetric potential energy function by the cross-correlated colored multiplicative noises at the cost of reduction of the asymmetric behavior of the system. The change of symmetry is mainly governed by the multiplicative noise-induced drift term. Thus external multiplicative noise can monitor a chemical reaction to understand the mechanism of the process.

We now check the validity of the unified colored noise approximation scheme. We have calculated a distribution function solving the Langevin equation (1) numerically using the Heun method [48]. It is a stochastic version of the Euler method, which reduces to the second order Runge-Kutta method in the absence of noise. Calculating the distribution function for a charged Brownian particle in the presence of a constant magnetic filed we have checked that this

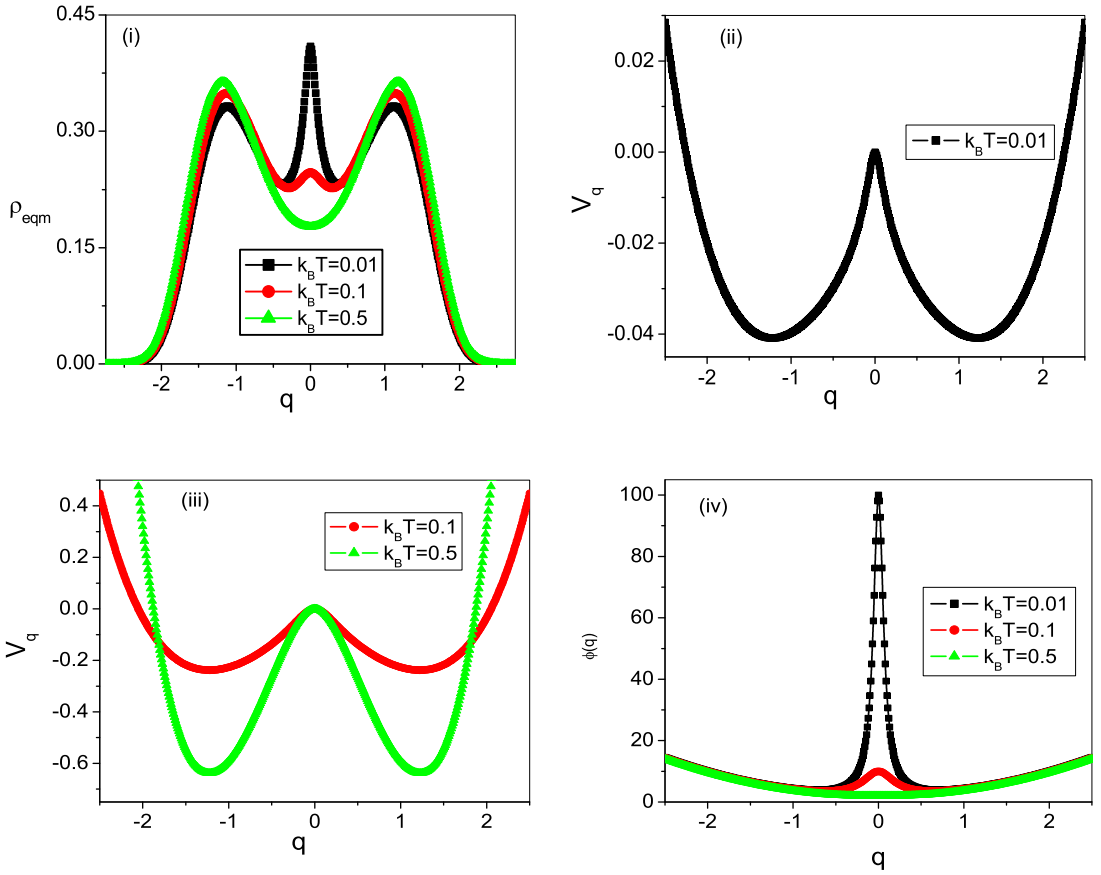

FIG. 2. (Color online) (i) Plot of distribution function vs coordinate for the parameter set $a = 0.25, b = 0.5, \gamma = 1.0$, $d_1 = d_2 = 0.5, \tau = \tau_1 = \tau_2 = 1.0, \lambda = 1.0$. The same parameter set is used for the other subfigures. (ii) Plot of the renormalized potential energy function $[V_q(q)]$ vs coordinate. (iii) Plot of the renormalized potential energy function $[V_q(q)]$ vs coordinate. (iv) Plot of $\phi(q)$ vs coordinate (units are arbitrary).

method gives a very accurate result [49]. To solve the stochastic differential equation we have used an integration step length 0.001. However, for different sets of parameters for a multiplicative noise-driven system we have calculated the distribution function numerically and compared with the approximate calculation in Fig. 1(iv). It shows a very good agreement between theory and numerical experiment. Then one may get further motivation to study another aspect like calculation of the mean first passage time as well as the barrier-crossing rate constant using this approximate description. The shape of the distribution function is strongly governed by the cross-correlation strength and noise correlation time of the colored multiplicative noises-driven open systems. It implies that these noise parameters may have a strong role in controlling the barrier-crossing rate along with the equilibrium population. In the next section we will explore barrier-crossing dynamics.

We now demonstrate how the distribution function (17) depends on the temperature. In Fig. 2 we have plotted the distribution function for different temperatures. It suggests that the particle is more localized at the transition point as the temperature of the system goes down. To understand this we have rearranged the distribution function (17) into the following form:

$$\rho_{eqm}(q) = N\phi(q)\exp\left[-\frac{V_q(q)}{D_T}\right], \tag{21}$$

where

$$\phi(q) = \frac{A(q)^2}{(D_e q^2 + D_T)} \tag{22}$$

and

$$V_q(q) = -\int_0^q \frac{[h(q')A(q') + D_e q']A(q') - A'(q')(D_e q'^2 + D_T)}{A(q')\left(\frac{D_e' q^2}{D_T} + 1\right)}\, dq'. \tag{23}$$

It is implied in Eq. (22) that $\phi(q)$ in the distribution function is the inverse of the position-dependent diffusion coefficient. $V_q(q)$ in Eq. (21) may be interpreted as the renormalized potential energy function for the system. In Fig. 2, we have demonstrated how $\phi(q)$ and $V_q(q)$ depend on the temperature. It shows that at a low-temperature limit,

the position-dependent diffusion coefficient (DC) around the barrier top is very small. As the particle moves away from the origin, the DC first increases to an optimum value and then monotonically decreases to a zero value. The particle may be localized at the barrier top of the renormalized double-well potential (as implied in both Figs. 1–2) by virtue of very weak diffusion at this point. The very nonmonotonous behavior of the diffusion process creates two minima around the barrier top in the variation of the probability distribution function as a function of the coordinate. There are two maxima around the two minima. These are certainly corresponding to the minima of the double-well potential. Thus the origin of the central maximum is quite different from the the other two, and the tristability is the signatures of both the position-dependent diffusion coefficient and the double-well potential. We now consider another limit. If the temperature is appreciably large, then the diffusion coefficient monotonically decreases as the particle moves away from the origin. Therefore the probability of finding a particle at the barrier top may be lower compared to its value at the minima of the double-well potential. Thus in the presence of colored multiplicative noises, the temperature of the thermal bath has an important role to contort the shape of the probability distribution function.

III. BARRIER-CROSSING DYNAMICS OF COLORED MULTIPLICATIVE NOISE-DRIVEN OPEN SYSTEMS

To determine the role of interference between the multiplicative noises on the barrier-crossing rate we have calculated the mean first passage time ($\langle T\rangle$, MFPT) [50] based on the Fokker-Planck equation (15). For the present problem it can be read as

$$\langle T_m\rangle(q_b|-q_b)=\int_{-q_b}^{q_b}dq\,\frac{\int_0^q\rho_{eqm}(q')\,dq'}{(D_eq^2+D_T)\rho_{eqm}(q)}. \tag{24}$$

This is the mean time which is required for a Brownian particle to travel the path from the minimum of the left well ($-q_b$) to the other minimum at the right well (q_b) for the first time. If the colored noises in Eq. (1) are additive in nature, then the above expression becomes

$$\langle T_a\rangle(q_b|-q_b)=\int_{-q_b}^{q_b}dq\,\frac{\int_0^q\rho_{eqa}(q')\,dq'}{(D_e+D_T)\rho_{eq}(q)}. \tag{25}$$

The expressions for the rate constant corresponding to above equations are

$$k_m=\frac{1}{\langle T_m\rangle(q_b|-q_b)} \tag{26}$$

and

$$k_a=\frac{1}{\langle T_a\rangle(q_b|-q_b)}. \tag{27}$$

To get an idea about the dependence of k_m or k_a on various parameters of the system we will calculate these using an approximate method. To begin we consider the Fokker-Planck equation (8) at a long time limit. It can be rearranged as

$$-\frac{\partial j}{\partial t}=0, \tag{28}$$

where

$$j=\frac{h(q)}{A}\rho(q)-\frac{D_eq\rho(q)}{A^2}-Q\frac{d\rho(q)}{dq} \tag{29}$$

with

$$Q=\frac{\left(c_fD_eq_f^2+D_T\right)}{A(q_f)^2} \tag{30}$$

and $A(q_f)=1-c_{f1}\tau_e[h'(q)-h(q)/q]$. Here q_f is the particle's position at a fixed point around which dynamics has been considered. To compensate the approximate description for Q and A, we have included parameters c_f and c_{f1} for best fit of the approximate results with the numerical experiment. Now Eq. (29) can be rewritten as

$$\frac{d\rho(q)}{dq}+\frac{V'(q)}{QA\gamma}\rho(q)+\frac{D_eq\rho(q)}{QA^2}=-\frac{j}{Q}. \tag{31}$$

Multiplying the integrating factor, $e^{\frac{V(q)}{QA\gamma}+\frac{D_eq^2}{2QA^2}}$, in the both sides of the above equation and then integrating the above equation between $-q_b$ and B we have

$$\left\{\rho(q)\exp\left[\frac{V(q)}{QA\gamma}+\frac{D_eq^2}{2QA^2}\right]\right\}_{-q_b}^{B}=-\frac{j}{Q}\int_{-q_b}^{B}\exp\left[\frac{V(q)}{QA\gamma}+\frac{D_eq^2}{2QA^2}\right]dq. \tag{32}$$

The constant current or flux across the barrier top (q_0) is thus

$$j=-Q\left\{\rho(q)\exp\left[\frac{V(q)}{QA\gamma}+\frac{D_eq^2}{2QA^2}\right]\right\}_{q_b}^{B}\times\int_{-q_b}^{B}\exp\left[\frac{V(q)}{QA\gamma}+\frac{D_eq^2}{2QA^2}\right]dq. \tag{33}$$

At the right side of the barrier top $\rho(q)$ is zero, i.e., $\rho(B)=0$. Then the above equation becomes

$$j=Q\left\{\rho(-q_b)\exp\left[\frac{V(-q_b)}{Q(-q_b)A(-q_b)\gamma}+\frac{D_eq_b^2}{2Q(-q_b)A(-q_b)^2}\right]\right\}\int_{-q_b}^{B}\exp\left[\frac{V(q)}{QA\gamma}+\frac{D_eq^2}{2QA^2}\right]dq. \tag{34}$$

Our next task is determination of the population at left well (n_a) at a zero current situation. Using the solution of Eq. (31) we have

$$n_a=\rho(-q_b)\exp\left[\frac{V(-q_b)}{Q(-q_b)A(-q_b)\gamma}+\frac{D_eq_b^2}{2Q(-q_b)A(-q_b)^2}\right]\times\int_{q_1}^{q_2}dq\exp\left[\frac{V(q)}{QA\gamma}+\frac{D_eq^2}{2QA^2}\right]. \tag{35}$$

Using Eqs. (34)–(35) one can write the expression for approximate rate constant (k_{am}) as

$$k_{am}=\frac{Q}{\int_{-q_b}^{B}\exp\left[\frac{V(q)}{QA\gamma}+\frac{D_eq^2}{2QA^2}\right]dq\int_{q_1}^{q_2}dq\exp\left[\frac{V(q)}{QA\gamma}+\frac{D_eq^2}{2QA^2}\right]}. \tag{36}$$

To evaluate the integrals in the above equation the potential function around the barrier top and the minimum of the left well can be approximated as

$$V(q) = V(q_0) - \tfrac{1}{2}\omega_b^2(q-q_0)^2 \tag{37}$$

and

$$V(q) = V(q_b) + \tfrac{1}{2}\omega_0^2(q-q_b)^2, \tag{38}$$

respectively. Here ω_b and ω_0 are the frequencies at the barrier top and the minima of the potential energy function, respectively. Using the above relations in Eq. (36) we have

$$k_{am} = \frac{\sqrt{a_0 a_b}}{\pi} e^{-\frac{\Delta E}{Q_0}} e^{-\frac{\Delta E_1}{Q_0}}, \tag{39}$$

where $a_0 = \frac{\omega_0^2}{2A_0\gamma} + \frac{D_e}{2A_0^2} = \frac{2b}{A_0\gamma} + \frac{D_e}{2A_0^2}$, $A_0 = A(-q_b) = 1 + \frac{\omega_0^2\tau_e}{\gamma} = 1 + \frac{4b\tau_e}{\gamma}$, $a_b = \frac{\omega_b^2}{2A_b\gamma} - \frac{D_e}{2A_b^2} = \frac{b}{A_b\gamma} - \frac{D_e}{2A_b^2}$, $A_b = A(q_0) = 1$, $\frac{\Delta E}{Q_0} = \frac{V(q_0)}{A_bQ_b\gamma} - \frac{V(-q_b)}{A_0Q_0\gamma} = \frac{b^2}{4aA_0Q_0\gamma}$, $Q_0 = Q(-q_b) = \frac{\frac{D_eb^2}{2a}+D_T}{A_0^2} = k_BT\frac{\frac{\gamma D_eb^2}{2ak_BT}+1}{\gamma A_0^2}$, $\frac{\Delta E_1}{Q_0} = \frac{b^2}{aA_0Q_0\gamma} - \frac{2b^3}{A_0^2Q_0\gamma^2a_0a}$. Here we have used $q_0 = 0, q_b = -\sqrt{\frac{b}{2a}}, \omega_0^2 = 4b$ and $\omega_b^2 = 2b$. The expression for the rate constant can be further simplified to have a better impression as

$$k_{am} = \frac{\sqrt{a_0 a_b}}{\pi} e^{-\frac{\Delta E_0 \times \Delta E_{cf}}{k_BT}}, \tag{40}$$

where $\Delta E_0 = V(q_0) - V(-q_b) = \frac{b^2}{4a}$ and $\Delta E_{cf} = \frac{2A_0ak_BT(4A_0b+5D_e\gamma)}{(4A_0b+D_e\gamma)(2ak_BT+D_eb^2\gamma)}$. We now check whether the above expression reduces to the standard result or not at the specific limit. First, we consider that $D_e = 0.0$ and $\tau_e = 0.0$. For this limit Eq. (40) becomes

$$k_{am} = \frac{\omega_0\omega_b}{2\pi\gamma} e^{-\frac{\Delta E_0}{k_BT}}. \tag{41}$$

Equation (41) is the well-known Kramers result at overdamped limit [51]. Thus it is a good check of our calculation. At the same time, the above equation implies how the frequency factor and activation energy depend on properties of cross-correlated multiplicative noises. It also implies the role of temperature and damping strength in this context.

We now consider the additive cross-correlated colored noises in the presence of thermal noise. Following the above prescription one can write the expression for the rate constant for the present case as

$$k_{aa} = \frac{\sqrt{a_0 a_b}}{\pi} e^{-\frac{\Delta E_0}{\gamma A_0 Q_0}} = \frac{\sqrt{a_0 a_b}}{\pi} e^{-\frac{\Delta E_0 \Delta E_{cf1}}{k_BT}}, \tag{42}$$

where $a_0 = \frac{\omega_0^2}{2A_0\gamma} = \frac{2b}{A_0\gamma}$, $A_0 = A(-q_b) = 1 + \frac{\omega_0^2\tau_e}{\gamma} = 1 + \frac{4b\tau_e}{\gamma}$, $a_b = \frac{\omega_b^2}{2A_b\gamma} = \frac{b}{A_b\gamma}$, $A_b = A(q_0) = 1 - \frac{\omega_b^2\tau_e}{\gamma}$, $Q_0 = Q(-q_b) = \frac{D_e+D_T}{A_0^2} = k_BT\gamma\frac{\frac{\gamma D_e}{k_BT}+1}{(1+4b\tau_e)^2}$, and $\Delta E_{cf1} = \frac{k_BT(\gamma+4b\tau_e)}{\gamma(k_BT+D_e\gamma)}$.

Finally, we consider another limit, $D_2 = 0.0, \tau_2 = 0.0$, and $k_BT \to 0$. Then $D_e = \frac{D_1}{\gamma^2}$ and $\tau_e = \tau_1$. For this condition Eq. (42) becomes

$$k_{aa} = \frac{\sqrt{2}b}{\pi\gamma}\sqrt{\frac{1}{A_0A_b}} e^{-\frac{\Delta E_0(\gamma+4b\tau_1)}{D_1}}. \tag{43}$$

For $\gamma = 1.0$ and $b\tau_1 \ll 1$, then the above relation takes the following form:

$$k_{aa} = \frac{\sqrt{2}b}{\pi}\sqrt{\frac{1}{1+2b\tau_1}} e^{-\frac{\Delta E_0(1+4b\tau_1)}{D_1}}. \tag{44}$$

We mention that the pre-exponential factor in the above expression is similar to the frequency factor of the rate constant, which was determined in Ref. [40], and the exponential factor (EF) in Eq. (44) is very close to the EF in the barrier-crossing rate which was calculated in Ref. [41]. Thus the present method is a unified approach.

Before leaving this part we would like to discuss the dependence of the rate constant on the strength of the cross-correlation and the noise correlation time of the external noises. As a signature of multiplicative noise-induced drift term, the frequency factor in the rate constant [Eq. (40)] depends on the strength of the multiplicative noise. Another usual role of the noise strength is to control the probability (through energy input) at top of the barrier against the dissipation for the open system. Thus activation energy depends on damping strength and noise intensity as indicated by Eqs. (40) and (42) for additive and multiplicative noise-driven processes, respectively. We now consider the role of noise correlation time in the present context. The memory effect of the external noise introduces the correlated motion of the Brownian particle like the deterministic force. As a signature of this, the frequency factor of the rate constant depends on the noise correlation time of the colored noise. Another role of the noise correlation time is that it enhances the effective barrier height through the reduction of the noise variance. Since the effective noise strength and noise correlation time depend on the nature of the cross-correlation among the noises, the rate constant depends on both the strength and the correlation time of the cross-correlation. The present discussion may be helpful in understanding the result, which will be demonstrated in the following subsections.

A. Breakdown of the Arrhenius result in the presence of the external noises

We now demonstrate how the rate constant depends on the temperature of the thermal bath. Using Eq. (26), we have calculated the rate constant (k_m) as a function of temperature for different noise parameters and plotted in Fig. 3. It shows that a breakdown of the Arrhenius result [51] occurs in the presence of colored multiplicative noise. One can account for it based on the approximate calculation. Equation (40) implies how the activation energy is influenced by the temperature of the thermal bath in the presence of colored multiplicative noises. The approximate calculation is corroborated by the exact calculation of the rate constant. A numerically calculated barrier-crossing rate has been presented in Fig. 6(i). It also implies a breakdown of the Arrhenius result in the presence of colored multiplicative noise. Thus the external noise-induced temperature dependent activation energy leads to the deviation from the Arrhenius result. For a given noise correlation time, the deviation is enhanced by the increase of strength of the cross-correlation or the intensity of the noises. It is manifested in the figure by the temperature independence on the rate

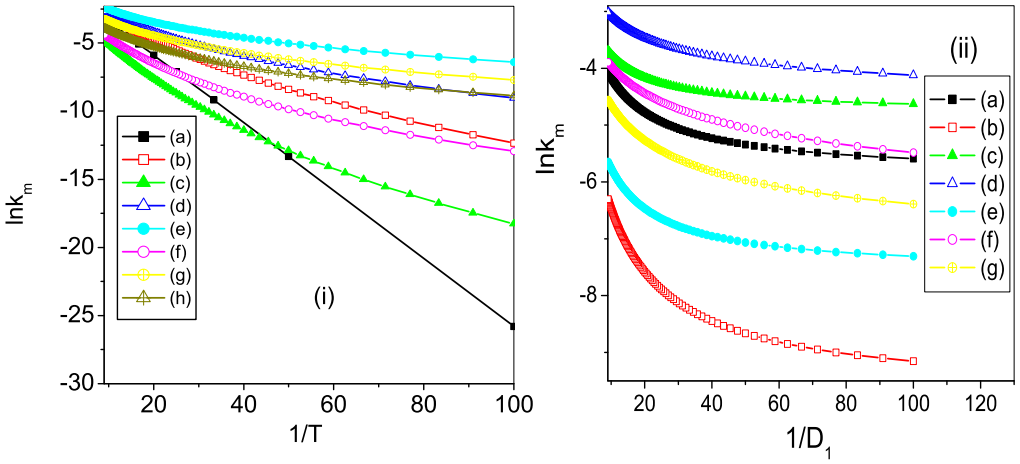

FIG. 3. (Color online) (i) Plot of $\ln k_m$ vs $1/T$ for the common parameter set $a = 0.25, b = 0.5, k_B = \gamma = 1.0$ and the following cases: (a) $d_1 = d_2 = 0.0, \tau = \tau_1 = \tau_2 = 0.0, \lambda = 0.0$; (b) $d_1 = 0.05, d_2 = 0.0, \tau = \tau_1 = \tau_2 = 0.0, \lambda = 0.0$; (c) $d_1 = 0.05, d_2 = 0.0, \tau_1 = 1.0, \tau = \tau_2 = 0.0, \lambda = 0.0$; (d) $d_1 = 0.05 = d_2, \tau_1 = \tau = \tau_2 = 0.0, \lambda = 0.0$; (e) $d_1 = 0.05 = d_2, \tau_1 = \tau = \tau_2 = 0.0, \lambda = 0.0$; (f) $d_1 = 0.05 = d_2, \tau_1 = \tau_2 = 1.0, \lambda = \tau = 0.0$; (g) $d_1 = 0.05 = d_2, \tau_1 = \tau_2 = 1.0, \lambda = 1.0, \tau = 0.0$; (h) $d_1 = 0.05 = d_2, \tau_1 = \tau_2 = 1.0, \lambda = 1.0 = \tau$. (ii) Plot of $\ln k_m$ vs $1/D_1$ for the common parameter set $a = 0.25, b = 0.5, k_B T = 0.05, \gamma = 1.0$ and the following cases: (a) $d_2 = 0.0, \tau = \tau_1 = \tau_2 = 0.0 = \lambda$; (b) $d_2 = 0.0, \tau_1 = 1.0, \tau = \tau_2 = 0.0 = \lambda$; (c) $d_2 = 0.05, \tau_1 = \tau = \tau_2 = 0.0 = \lambda$; (d) $d_2 = 0.05, \tau_1 = \tau = \tau_2 = 0.0, \lambda = 1.0$; (e) $d_2 = 0.05, \tau_1 = \tau_2 = 1.0, \tau = \lambda = 0.0$; (f) $d_2 = 0.05, \tau_1 = \tau_2 = 1.0, \tau = 0, \lambda = 1.0$; (g) $d_2 = 0.05, \tau_1 = \tau_2 = 1.0, \tau = \lambda = 1.0$ (units are arbitrary).

constant at a low temperature regime. At this limit, the effect of temperature on the barrier-crossing rate becomes insignificant compared to the strength of external noises, which is implied in Eq. (40). On the other hand if the noise becomes more colored for the given values of the strength of cross-correlation or noise intensity, then the extent of deviation is reduced, particularly at low-temperature regime.

In the next step, based on Eq. (26) we have demonstrated the dependence of the rate constant on the strength of the multiplicative noise in Fig. 3(ii). It is apparent in this figure that $\ln k_m$ is a nonlinear function of $\frac{1}{D_1}$. Deviation from the linear behavior is strong at relatively higher noise strength. This nonlinear behavior is implied in Eq. (40) through the appearance of D_1 in both the frequency factor and the activation energy. It is a signature of the multiplicative noise-induced drift term, which is a function of the noise strength.

B. The deviation of the rate constant from the power law behavior as a function of damping strength in the presence of external noise

Equations (40) and (41) imply that the rate constant as a function of damping strength deviates from the power law [51] in the presence of the multiplicative noises. Based on Eq. (26) the role of noise properties on the deviation is demonstrated in Fig. 4(i). The curves (g) and (h) in the figure imply that as the noise becomes more colored, then the deviation from the power law is stronger. One can interpret it physically that the effect of

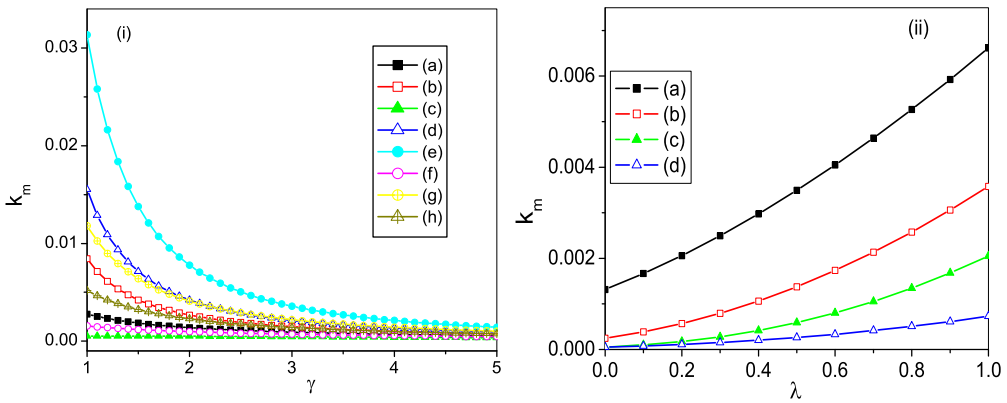

FIG. 4. (Color online) (i) Plot of k_m vs γ for the common parameter set $a = 0.25, b = 0.5, k_B T = 0.05$ and the following cases: (a) $d_1 = d_2 = 0.0, \tau = \tau_1 = \tau_2 = 0.0, \lambda = 0.0$; (b) $d_1 = 0.05, d_2 = 0.0, \tau = \tau_1 = \tau_2 = 0.0, \lambda = 0.0$; (c) $d_1 = 0.05, d_2 = 0.0, \tau_1 = 1.0, \tau = \tau_2 = 0.0, \lambda = 0.0$; (d) $d_1 = 0.05 = d_2, \tau_1 = \tau = \tau_2 = 0.0, \lambda = 0.0$; (e) $d_1 = 0.05 = d_2, \tau_1 = \tau = \tau_2 = 0.0, \lambda = 1.0$; (f) $d_1 = 0.05 = d_2, \tau_1 = \tau_2 = 1.0, \lambda = \tau = 0.0$; (g) $d_1 = 0.05 = d_2, \tau_1 = \tau_2 = 1.0, \lambda = 1.0, \tau = 0.0$; (h) $d_1 = 0.05 = d_2, \tau_1 = \tau_2 = 1.0, \lambda = 1.0 = \tau$. (ii) Plot of k_m vs strength of cross-correlation (λ) for the common parameter set $a = 0.25, b = 0.5, k_B T = 0.02, \gamma = 1.0, d_1 = 0.05 = d_2$. (a) $\tau = \tau_1 = \tau_2 = 0.0$; (b) $\tau_1 = 1.0, \tau = \tau_2 = 0.0$; (c) $\tau_1 = 1.0 = \tau_2, \tau = 0.0$; (d) $\tau_1 = 1.0 = \tau_2 = \tau$ (units are arbitrary).

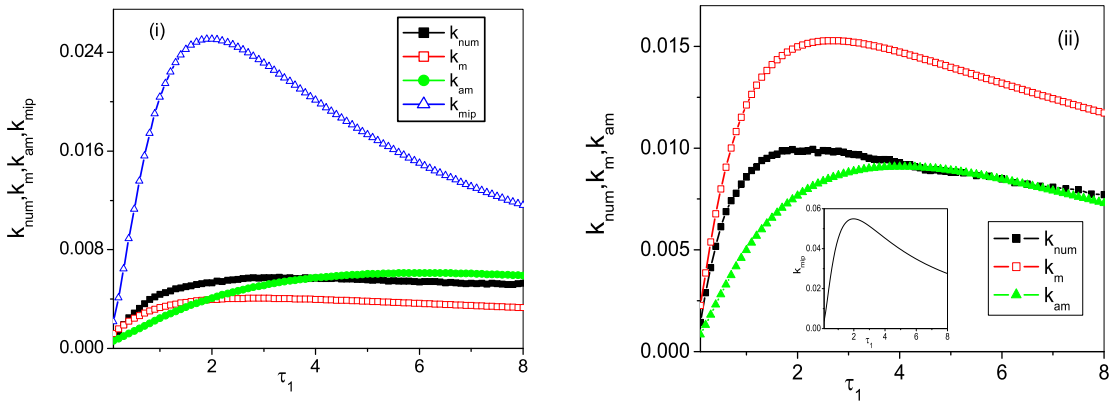

FIG. 5. (Color online) Plot of $k_{\rm num}, k_m, k_{am}, k_{mip}$ vs τ_1 for fixed variance and the common parameter set $a = 0.25, b = 0.5, k_B T = 0.04, \gamma = 1.0$. (i) $c_0 = 0.1, \lambda = 0.0$, $c_f = 0.25, c_{f1} = 0.06$. (ii) $c_0 = 0.1, \lambda = 1.0, c_f = 0.25, c_{f1} = 0.1$. In the inset we have plotted k_{mip} vs τ_1 for fixed variance with the same parameter set as in the main figure (units are arbitrary).

damping strength on the diffusion is reduced for the decrease of noise fluctuations with increase in noise correlation time. Thus if the cross-correlation is white, then deviation from the power law is small compared to the colored cross-correlation situation.

C. The behavior of the rate constant as a function of strength of the interference between the noises

The strength of the cross-correlation among the noises affects both the effective noise strength and the correlation time of the stochastic process. Its control on the rate constant through these quantities has been demonstrated in Fig. 4(ii). This figure shows that the barrier-crossing rate increases as a nonlinear function of the strength of the interference between the noises. It is a signature of increase of effective noise strength and decrease of noise correlation time with the enhancement of the strength of the interference. The growth rate reduces as the individual noises and their cross-correlation become colored. It may be due to an insignificant decrease of effective noise correlation time with the increase of λ. Another point to be mentioned here is the increase of the rate constant as a function of strength of cross-correlation in the present system is behavior in contrast to that in Ref. [29]. In other words, if one of the cross-correlated noises becomes additive, then the rate constant decreases as the strength of the interference grows.

D. The cross-correlation-induced resonant activation

During the last two decades it has been observed that the exploring of the resonant activation phenomenon has been a key issue in the field of barrier-crossing dynamics. In this context, we have examined the role of noise cross-correlation. In Fig. 5 we have demonstrated the variation of the rate constant as a function of effective noise correlation time for a given noise variance. Thus for this plot the effective noise strength (D_e) and τ_e obey the following relationship:

$$D_e = 2c_0(1+\lambda)\tau_e. \tag{45}$$

One can achieve the above relation easily by the simple choice, $D_2 = D_1 = c_0\tau_1$ and $\tau = \tau_2 = \tau_1$. For $D_2 = 0$, relation (45) becomes

$$D_e = D_1 = c_0\tau_e = c_0\tau_1. \tag{46}$$

The above equation is generally considered to study the resonant activation behavior [15,18,19,52]. However, it is apparent in Fig. 5 that colored cross-correlation may induce resonant activation. For the given parameter set the resonant activation phenomenon almost disappears in the absence of cross-correlation. Then the rate constant increases nearly monotonically as a function of noise correlation time. Here enhancement of the barrier-crossing rate due to increase of noise strength dominates over the suppression of the rate constant by the noise correlation time [18]. To check the validity of the unified colored noise approximation we have presented the result from the numerical experiment in Fig. 5. We have calculated the barrier-crossing rate numerically using the earlier mentioned procedure. For the multiplicative noise-driven case, we have represented the numerical result by $k_{\rm num}$. In the same figure we have also presented the result, which is calculated following the interpolation method [46]. According to this method, $\frac{1}{A}$ in Eq. (9), has to be replaced by

$$\frac{1}{A_{ipa}} = \frac{1 - c[\tau_e h'(q)]^{n-1}}{1 + c[\tau_e h'(q)]^n}. \tag{47}$$

c and n in the above equation are adjustable parameters for the best fit of a particular experimental data. It is noted here that the above equation reduces to Eq. (9) for $c = -1$ and $n = 2$. It is difficult to develop the interpolation scheme for the multiplicative noise-driven case. We assume a similar kind of function like A_{ipa} for A in Eq. (7), and it is represented by

$$\frac{1}{A_{ipm}} = \frac{1 - c\{\tau_e[h'(q) - h(q)/q]\}^{n-1}}{1 + c\{\tau_e[h'(q) - h(q)/q]\}^n}. \tag{48}$$

If we replace A in Eq. (26) by A_{ipm}, then k_m is substituted by k_{mip}. It is surprising to note that the very approximate calculation based on the above function qualitatively agrees with the numerical result as shown in Fig. 5(ii). Here another issue to be mentioned that $c = 0.44$ and $n = 2$ are corresponding to the best fit of theoretical result with the numerical experiment. This choice has been considered for the additive noise-driven case in Ref. [46]. We have also checked

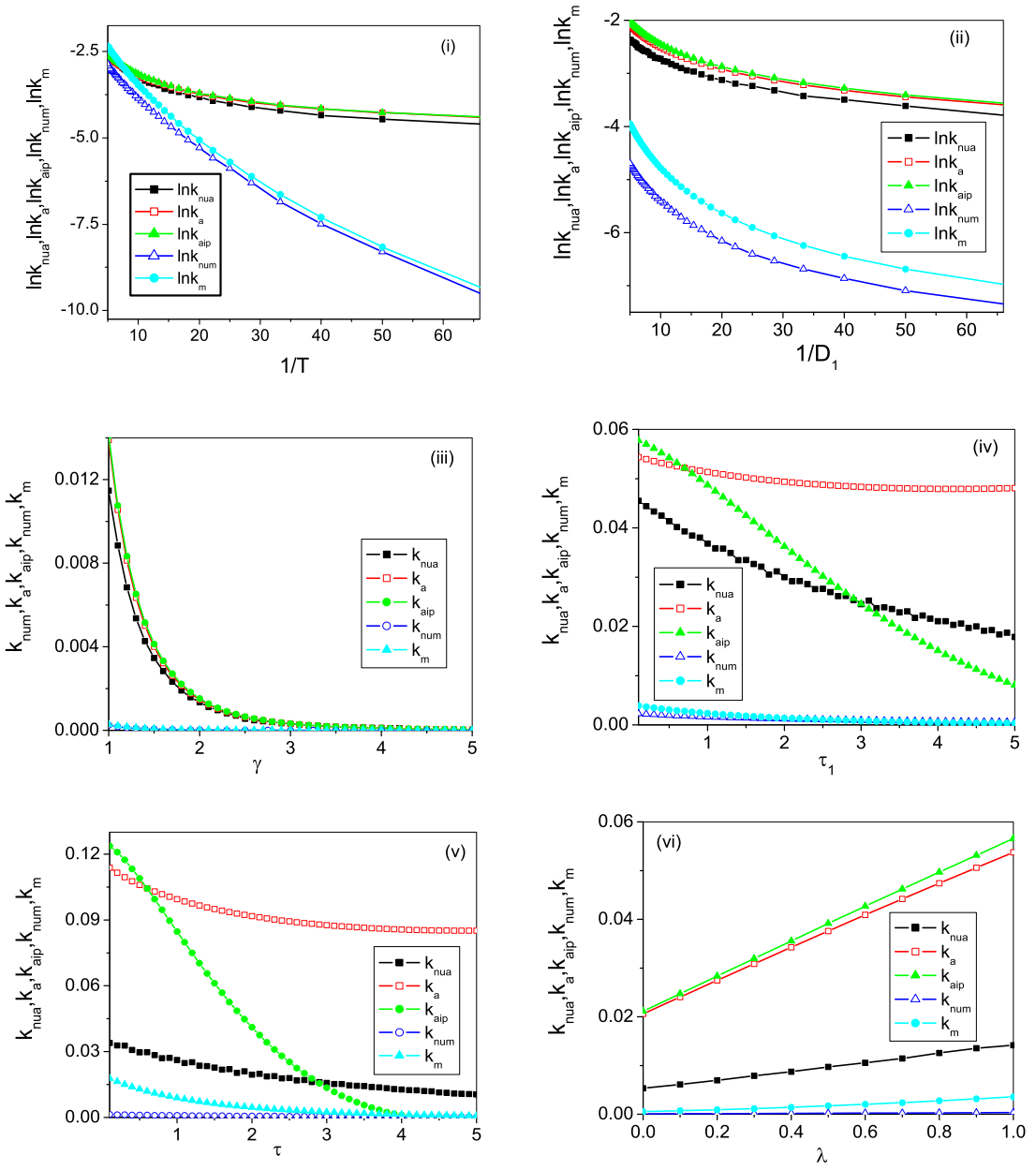

FIG. 6. (Color online) (i) Plot of $\ln k_{\rm nua}$, $\ln k_a$, $\ln k_{\rm aip}$, $\ln k_{\rm num}$ and $\ln k_m$ vs $1/T$ for the parameter set $k_B = \gamma = 1.0, d_1 = d_2 = 0.02, \tau = \tau_1 = \tau_2 = 0.25, \lambda = 1.0$. (ii) Plot of $\ln k_{\rm nua}$, $\ln k_a$, $\ln k_{\rm aip}$, $\ln k_{\rm num}$ and $\ln k_m$ vs $1/D_1$ for the parameter set $k_BT = 0.02, d_2 = 0.05, \tau = \tau_1 = \tau_2 = 0.25, \lambda = 1.0$. (iii) Plot of $k_{\rm nua}$, k_a, $k_{\rm aip}$, $k_{\rm num}$ and k_m vs γ for the parameter set $k_BT = 0.02, d_1 = d_2 = 0.02, \tau = \tau_1 = \tau_2 = 0.25, \lambda = 1.0$. (iv) Plot of $k_{\rm nua}$, k_a, $k_{\rm aip}$, $k_{\rm num}$ and k_m vs τ_1 for fixed noise strength and the parameter set $k_BT = 0.02, d_1 = d_2 = 0.05, \tau = \tau_2 = 0.25, \lambda = 1.0$. (v) Plot of $k_{\rm nua}$, k_a, $k_{\rm aip}$, $k_{\rm num}$ and k_m vs τ for fixed noise strength and the parameter set $k_BT = 0.02, d_1 = d_2 = 0.05, \tau_1 = \tau_2 = 0.25, \lambda = 1.0$. (vi) Plot of $k_{\rm nua}$, k_a, $k_{\rm aip}$, $k_{\rm num}$ and k_m vs strength of cross-correlation (λ) for the parameter set, $k_BT = 0.02, d_1 = d_2 = 0.05, \tau = \tau_1 = \tau_2 = 0.25$ (units are arbitrary).

that it is the best choice for an additive colored cross-correlated noise-driven system for any parameter set. Shortly we will present the result for the additive noise-driven case. However, Fig. 5 implies that the pattern of the result which is calculated based on the unified colored noise approximation and the numerical result is quite similar for the wide range of noise intensity and correlation time. At the same time, this figure also suggests that at the small noise correlation time limit the scheme may be a good one. We will further check the validity of this method in the next subsection.

E. A comparative study of the rate constants for additive and multiplicative noise-driven cases

In this subsection we investigate how the rate constant changes if the multiplicative noises (MNs) become additive in nature. The dependence of the rate constant on the noise properties has been demonstrated in Fig. 6. For this figure we have chosen the common parameter set, $a = 0.25, b = 0.5$. It shows that the rate constant for a given set of parameters is significantly greater for the additive noises (AN)-driven process compared to the other case. This is implied in the

approximate calculation. The calculation suggests that the frequency factor for the AN-driven case is greater than that of the other. One can account for further details of Fig. 6 (such as a breakdown of the Arrhenius result being stronger for AN than that of MN) based on the earlier discussion and the approximate calculations. In this figure we have compared the numerical result with analytically calculated data. The numerically calculated barrier-crossing rate constant for additive colored noise-driven case is denoted by k_{nua}. In Fig. 6 k_{aip} corresponds to the rate constant, which has been calculated using A_{ipa} in Eq. (27). However, Fig. 6 suggests that sometimes the interpolation method is better than that of the unified colored noise approximation scheme. Thus searching for an interpolation-like scheme for the multiplicative colored noise-driven case may be an important issue in the near future.

IV. CONCLUSION

Based on the Fokker-Planck description of the stochastic process we have studied properties of the cross-correlated colored noise-driven dynamical system. To make the present study general we have considered that the noise may be either additive or multiplicative in nature. Here we present a comparative study based on the two cases. Our major observations include the following points.

(i) The transition state of the double-well potential can be stabilized by the introduction of colored cross-correlation between the multiplicative noises. This can be achieved for the asymmetric double-well potential also at the cost of reduction of the asymmetric behavior of the system. Thus the external multiplicative noises can monitor a chemical reaction to understand the mechanism of the process.

(ii) Breakdown of the Arrhenius result occurs in the presence of multiplicative noise. For the cross-correlated noises it becomes stronger. If the cross-correlation or noises become colored, then the extent of the breakdown reduces. Furthermore, for a given noise parameter set the breakdown is strong for the additive noise compared to the other case. Here it should be noted that the rate constant is higher for additive noise compared to multiplicative noise. The Arrhenius-like plot for the variation of rate constant as a function of the strength of the external noise is a nonlinear type. The nonlinearity is strong for multiplicative noise compared to additive noise.

(iii) Deviation from the power law behavior of the rate constant as a function of damping strength is stronger if the noise becomes more colored. Thus if the cross-correlation is white, then deviation from the power law is small compared to the colored cross-correlation situation.

(iv) There is a cross-correlation induced resonant activation for the colored multiplicative noises-driven system.

(v) Barrier-crossing rate increases with increase in cross-correlation strength. The growth rate enhances as the interference between the noises becomes stronger. If the individual noises and their cross-correlation become colored, then the growth rate is reduced. Furthermore, increase of the rate constant in the present system is in sharp contrast to the case where one of the cross-correlated noises is additive in nature [29].

(vi) Finally, comparing the present calculation with the earlier studies in Refs. [40,41] one may conclude that the present method is a unified approach.

(vii) A comparative study suggests that sometimes the interpolation method is better than that of the unified colored noise approximation scheme. Thus searching for an interpolation-like scheme for the multiplicative colored noise-driven case may be an important issue in the near future.

[1] N. G. van Kampen, Prog. Theor. Phys. **64**, 389 (1978).

[2] C. W. Gardiner, *Handbook of Stochastic Methods for Physics, Chemistry, and the Natural Science* (Springer-Verlag, Berlin, 1983).

[3] H. Risken, *The Fokker-Planck Equation: Methods of Solution and Applications* (Springer-Verlag, Berlin, 1984).

[4] P. Hänggi, P. Talkner, and M. Borkovec, Rev. Mod. Phys. **62**, 251 (1990).

[5] V. I. Mel'nikov, Phys. Rep. **209**, 1 (1991).

[6] N. G. van Kampen, *Stochastic Processes in Physics and Chemistry*, 3rd ed. (Elsevier, Amsterdam, 2007).

[7] E. J. Allen, Dyn. Contin. Discrete Impulsive Sys. **5**, 271 (1999).

[8] N. T. J. Bailey, *The Elements of the Stochastic Processes with Applications to the Natural Sciences* (John Wiley and Sons, New York, 1990).

[9] A. Okubo and S. A. Levin, *Diffusion and Ecological Problems: Modern Perspectives* (Springer, New York, 2001).

[10] N. L. Stokey, R. E. Lucas, and E. C. Prescott, *Recursive Methods in Economic Dynamics* (Harvard University Press, Cambridge, MA, 1989).

[11] C. W. Gardiner, *Stochastic Methods: A Handbook for the Natural and Social Sciences*, Springer Series in Synergetics 2207 (Springer-Verlag, Berlin, Heidelberg, NY, 1986).

[12] P. K. Ghosh, M. K. Sen, and B. C. Bag, Phys. Rev. E **78**, 051103 (2008).

[13] M. K. Sen, S. Ray, A. Baura, and B. C. Bag, Chem. Phys. Lett. **559**, 117 (2013).

[14] F. Marchesoni and P. Grigolini, J. Chem. Phys. **78**, 6287 (1983); J. B. Straus and G. A. Voth, *ibid.* **96**, 5460 (1993); J. B. Straus, J. M. G. Llorente, and G. A. Voth, *ibid.* **98**, 4082 (1993); G. R. Haynes, G. A. Voth, and E. Pollak, *ibid.* **101**, 7811 (1994); J. Ray Chaudhuri, B. C. Bag, and D. S. Ray, *ibid.* **111**, 10852 (1999); D. Banerjee, B. C. Bag, and D. S. Ray, *ibid.* **120**, 8960 (2004); D. Barik, B. C. Bag, and D. S. Ray, *ibid.* **119**, 12973 (2003); B. C. Bag, *ibid.* **119**, 4988 (2003); B. C. Bag, C. K. Hu, and M. S. Li, Phys. Chem. Chem. Phys. **12**, 11753 (2010); P. K. Ghosh, M. S. Li, and B. C. Bag, J. Chem. Phys. **135**, 114101 (2011); A. Baura, S. Ray, M. K. Sen, and B. C. Bag, J. Appl. Phys. **113**, 124905 (2013); A. Baura, M. K. Sen, and B. C. Bag, Chem. Phys. **417**, 30 (2013); A. Baura, S. Ray, and B. C. Bag, J. Chem. Phys. **138**, 244110 (2013).

[15] S. Ray, D. Mondal, and B. C. Bag, J. Chem. Phys. **140**, 204105 (2014).

[16] L. Gammaitoni, P. Hänggi, P. Jung, and F. Marchesoni, Rev. Mod. Phys. **70**, 223 (1998).

[17] C. R. Doering and J. C. Gadoua, Phys. Rev. Lett. **69**, 2318 (1992).

[18] P. Majee, G. Goswami, and B. C. Bag, Chem. Phys. Lett. **416**, 256 (2005).
[19] P. K. Ghosh, D. Barik, B. C. Bag, and D. S. Ray, J. Chem. Phys. **123**, 224104 (2005).
[20] P. K. Ghosh, B. C. Bag, and D. S. Ray, J. Chem. Phys. **127**, 044510 (2007).
[21] S. K. Banik, J. Ray Chaudhuri, and D. S. Ray, J. Chem. Phys. **112**, 8330 (2000); A. Baura, M. K. Sen, G. Goswami, and B. C. Bag, *ibid.* **134**, 044126 (2011).
[22] F. Cottone, H. Vocca, and L. Gammaitoni, Phys. Rev. Lett. **102**, 080601 (2009); V. Me'ndez, D. Campos, and W. Horsthemke, Phys. Rev. E **88**, 022124 (2013).
[23] X. Luo and S. Zhu, Phys. Rev. E **67**, 021104 (2003).
[24] H. Hasegawa, Physica A **392**, 2532 (2013).
[25] M. Marchi, F. Marchesoni, L. Gammaitoni, E. Menichella-Saetta, and S. Santucci, Phys. Rev. E **54**, 3479 (1996).
[26] W. Horsthemke and R. Lefever, *Noise Induced Transition: Theory and Application in Physics, Chemistry and Biology* (Springer, Berlin, 1983).
[27] P. Reiman, Phys. Rep. **361**, 57 (2002).
[28] I. I. Fedchenia, J. Stat. Phys. **52**, 1005 (1988); A. Fulinski and T. Telejko, Phys. Lett A **152**, 11 (1991).
[29] A. J. R. Madureira, P. Hängi, and H. S. Wio, Phys. Lett. A **217**, 248 (1996)
[30] D. Mei, C. Xie, and L. Zhang, Phys. Rev. E **68**, 051102 (2003); P. Majee and B. C. Bag, J. Phys. A: Math. Gen. **37**, 3352 (2004); J. Ray Chaudhuri, S. Chattopadhyay, and S. K. Banik, J. Chem. Phys. **128**, 154513 (2008).
[31] J. Ray Chaudhuri, S. Chattopadhyay, and S. K. Banik, Phys. Rev. E **76**, 021125 (2007); J. Ray Chaudhuri, P. Chaudhury, and S. Chattopadhyay, J. Chem. Phys. **130**, 234109 (2009).
[32] S. Zhu, Phys. Rev. A **47**, 2405 (1993).
[33] Y. Jia and J. R. Li, Phys. Rev. E **53**, 5786 (1996).
[34] J. H. Li and Z. Q. Huang, Phys. Rev. E **57**, 3917 (1998); G. Goswami, P. Majee, P. K. Ghosh, and B. C. Bag, Physica A **375**, 249 (2007).
[35] V. Berdichevsky and M. Gitterman, Phys. Rev. E **60**, 1494 (1999); C. J. Tessone, H. S. Wio, and P. Hänggi, J. Chem. Phys. **62**, 4623 (2000).
[36] B. Q. Ai, X. J. Wang, G. T. Liu, and L. G. Liu, Phys. Rev. E **67**, 022903 (2003).
[37] B. C. Bag, S. K. Banik, and D. S. Ray, Phys. Rev. E **64**, 026110 (2001); B. C. Bag, *ibid.* **65**, 046118 (2002); **66**, 026122 (2002).
[38] Y. Jia and J.-R. Li, Phys. Rev. Lett. **78**, 994 (1997); K. P. Singh, G. Ropars, M. Brunel, and A. Le Floch, *ibid.* **90**, 073901 (2003).
[39] C. Wagner and T. Kiefhaber, Proc. Natl. Acad. Sci. USA **96**, 6716 (1999).
[40] P. Hänggi, F. Marchesoni, and P. Grigolini, Z. Phys. B **56**, 333 (1984).
[41] F. Marchesoni, Phys. Rev. A **36**, 4050 (1987).
[42] Y. Jia, S.-N. Yu, and J.-R. Li, Phys. Rev. E **62**, 1869 (2000).
[43] P. Hänggi and P. Jung, Adv. Chem. Phys. **89**, 239 (1995).
[44] C. Li, W. Da-jin, and K. Sheng-zhi, Phys. Rev. E **52**, 3228 (1995).
[45] P. Colet, H. S. Wio, and M. San Miguel, Phys. Rev. A **39**, 6094 (1989); H. S. Wio, P. Colet, M. San Miguel, L. Pesquera, and M. A. Rodriguez, *ibid.* **40**, 7312 (1989).
[46] F. Castro, H. S. Wio, and G. Abramson, Phys. Rev. E **52**, 159 (1995).
[47] E. Pollak and A. M. Berezhkovskiia, J. Chem. Phys. **99**, 1344 (1999).
[48] R. Toral, in *Computational Physics*, edited by P. Garrido and J. Marro, Lecture Notes in Physics, Vol. 448 (Springer-Verlag, Berlin, 1995).
[49] S. Mondal, S. Das, A. Baura, and B. C. Bag, J. Chem. Phys. **141**, 224101 (2014).
[50] K. Lindenberg and B. J. West, J. Stat. Phys. **42**, 201 (1986).
[51] H. A. Kramers, Physica (Utrecht) **7**, 284 (1940).
[52] P. Hänggi, Chem. Phys. **180**, 157 (1994); P. Reimann *et al.*, *ibid.* **235**, 11 (1998); B. C. Bag and C. K. Hu, Phys. Rev. E **73**, 061107 (2006); Chem. Phys. **75**, 042101 (2007); G. Goswami, P. Majee, P. K. Ghosh, and B. C. Bag, Physica A **374**, 549 (2007); G. Goswami, P. Majee, and B. C. Bag, Fluctuation Noise Lett. **7**, L151 (2007); M. K. Sen, A. Baura, and B. C. Bag, J. Stat. Mech.: Theory Exp. (2009) P11004.